Neurology Asia 2014; 19(3) : 241 – 247

ORIGINAL ARTICLES

Hemodynamic effects resulting from a common carotid to middle cerebral bypass with varying degrees of proximal internal carotid stenosis

[1]Sheau Fung Sia *MD PhD*, [2]Yu Zhang *PhD*, [3]Yi Qian *PhD*, [4]Khairul Azmi Abd Kadir *MRad*, [4]Hazman Mohd Nor *MRad*, [3]Michael Kerin Morgan *MD FRACS*

[1]Division of Neurosurgery, Surgery Department; [4]Department of Biomedical Imaging, Faculty of Medicine, University of Malaya, Kuala Lumpur, Malaysia; [2]Institute for Infrastructure Engineering, University of Western Sydney, Penrith, NSW; [3]The Australian School of Advanced Medicine, Macquarie University, North Ryde, NSW, Australia

Abstract

Objective: To investigate the degree of stenosis of the internal carotid artery required for continuous blood flow in an interposition vein bypass to the middle cerebral artery. *Methods:* Computational fluid dynamics techniques were used to investigate a case of common carotid to middle cerebral artery brain bypass with varying degrees of internal carotid artery stenosis. Blood flow patterns across the patient-specific brain bypass were evaluated. *Results:* Simulation found that for cross section stenosis of less than 60%, no flow occurred in the bypass graft. Further narrowing of the internal carotid artery increased flow linearly within the bypass graft. There was significant energy loss and pressure gradient difference between the proximal and distal anastomosis sites of the bypass.
Conclusion: Computational fluid dynamics helps us to quantify the flow distribution, wall shear stress and pressure gradient in brain bypass surgery. The angle of the distal anastomosis had no effect on hemodynamic indices, allowing this consideration to be ignored in modeling. This modeling technique is useful to estimate the required degree of stenosis in the artery that is to be occluded to ensure sustained flow in the bypass. This will be of importance where there is staged surgery with a time interval between the bypass and the definitive internal carotid artery occlusion.

INTRODUCTION

Brain bypass surgery can be performed to either augment or replace cerebral blood flow.[1] The choice of intracranial revascularization procedures are not standardized and depend on available conduits (arterial pedicle or venous graft), blood flow adequacy to the intended bypass territories, surgical technique complexity (end-to-side, end-to-end or side-to-side anastomosis), and the long-term expectations of graft patency.[1-7] In some cases, where vessel occlusion is anticipated for the need of treating a tumor or aneurysm, it may be decided to stage the procedures, with a time interval between establishing the bypass and the definitive occlusion or sacrifice of the vessel. However, the potential for the competition of flow by the native circulation may negatively impact upon the sustainability of the bypass graft. More precisely, presence of abnormally high or low shear rates through the bypass favors abnormal platelets activation, thrombus formation and graft failure.[8-11]

A strategy that can be used to induce and maintain the flow in the bypass is to surgically narrow the artery for occlusion at the time of the brain bypass procedure. However, the degree of narrowing necessary is poorly understood.

A second concern is the prediction of the consequences for the sharing of downstream flow between the bypass and the native collaterals (compensating the loss of normal blood supply). Surgically created anastomoses will induce local flow disturbances, alter velocity profiles[12] and will alter the internal borderzone between native collateral flow and bypass flow. At the boundaries between these territories, there will be a point with no or low flow. Where the bypass is established on the middle cerebral artery (MCA), such

Address correspondence to: Associate Professor Dr Sheau Fung Sia, MD PhD, Division of Neurosurgery, Surgery Department, Faculty of Medicine, University of Malaya, Kuala Lumpur, Malaysia. Tel: +60 (03) 7949 2149, Fax: + 60 (03) 7958 6360, Email: sfsia02@um.edu.my

points of low flow may occur in the region of the lenticulostriate arteries.[5] Internal borderzone infarctions may result from branch occlusion due to these hemodynamic changes.

The objective of this study was to demonstrate the feasibility of integrating patient-specific three-dimensional (3D) computed tomography angiography (CTA) image data to construct the patient-specific computational fluid dynamic (CFD) model of brain bypass anastomosis. A common carotid artery (CCA) to middle cerebral artery (MCA) bypass was modeled with varying degrees of internal carotid artery (ICA) stenosis. The modeling was used to predict the minimal degree of stenosis necessary to ensure sustained continuous flow in the bypass. This model was tested with varying angles of the distal anastomosis to see how this might affect the prediction. This was thought to be important, as the angle of the distal anastomosis cannot be easily predicted prior to surgery.

METHODS

A tall 13-year-old Marfanoid boy presented with progressive left visual loss over one year. He was diagnosed with a fusiform left ICA aneurysm. He underwent inter-position saphenous venous grafting (IPSVG) brain bypass from the left common carotid artery (CCA) to middle cerebral artery (MCA). At the same surgical procedure the intracranial ICA proximal to the aneurysm was surgically trapped and narrowed. The trapped ICA segment was not completely ligated in order to preserve a minimal flow to the ophthalmic artery to avoid sudden loss of retinal blood flow.

Our methods, and the computational hemodynamic analysis system, have been described in detail and validated in-vivo and in-vitro in previous studies.[13,14] In summary, the medical imaging data CTA was performed using a helical CT scanner (GE Medical Systems) with multidetector-row capability. A section thickness of 0.625mm, a table speed of 9mm/s and zero-degree table (and gantry tilt) were used. Sections in DICOM format were acquired with a 512 x 512 matrix. Scanning was started from the arch of the aorta and continued parallel to the orbito-meatal line to the level just beyond the Circle of Willis during the intravenous injection of contrast material at the rate of 3.5mls/s. All the images were immediately transferred to a workstation (Real-Intage®) for volume rendering. Contour interpolation was used to generate 2-D contours based on gray scales pixels with a thresholding value of 226 to 3071. Following this, a 3-D geometry was built by interpolating those 2-D contours in normal direction. The luminal surface of the vascular anastomosis in brain bypass surgery was extracted in the format suitable for import by grid generators, with each grid size maximum of 0.3mm. This method avoids surface noise that would result in inaccuracy of 3D geometry. Instead of using the global smoothing, we used manual local smoothing to keep the 3D geometry as realistic as possible. This method gave an average error of one third of original pixel size in 3D geometry.[15] Three-dimensional geometries were reconstructed for the purpose of flow simulation. Optimum number of grid nodes, with best accuracy and optimum computing time, were established using ANSYS workbench (V 12.1, ANSYS, Inc., USA) on cluster desktop computers. CFD was performed assuming a solid vessels vein graft wall and non-slip and non-penetration constraints at the wall. With the real-time velocities derived from pulse-doppler ultrasound displaying the spectrum of blood velocities, the mean arterial velocity was used as inlet boundary criteria. The simulation was performed under steady flow condition. Based on the patient CTA extraction of the vascular configuration data from the 90% stenosis of the ICA, various morphology bypass models were simulated looking at blood flow indices and wall shear stress (WSS) changes at the proximal and distal anastomoses following computer model reconstruction of the ICA with variations in the degree of stenosis (Figure 1) and anastomosis angles (150 °, 135 °, 90 ° and 75 °). The blood flow calculations performed by the computational analysis system of equations utilized the Navier-Stokes (N-S) equation and continuity equation (1) that describe the most general movement of fluid medium. These equations are defined below.

$$\begin{cases} \dfrac{\partial}{\partial x_i}(\rho u_i u_i) = -\dfrac{\partial p}{\partial x_i} + \dfrac{\partial}{\partial x_j}\left[\mu\left(\dfrac{\partial u_i}{\partial x_j} + \dfrac{\partial u_j}{\partial x_i}\right)\right] \\ \dfrac{\partial}{\partial x_j}(\rho u_j) = 0 \end{cases} \quad (1)$$

where i, j=1,2,3, x_1, x_2, x_3 means coordinate axes, u_i, u_j and p are the velocity vector and the pressure in the point of the fluid domain, ρ and μ are blood density and viscosity. Due to the relative large size of the vessels compared to individual blood cells and typically large shear rates in arteries, the blood flows were assumed

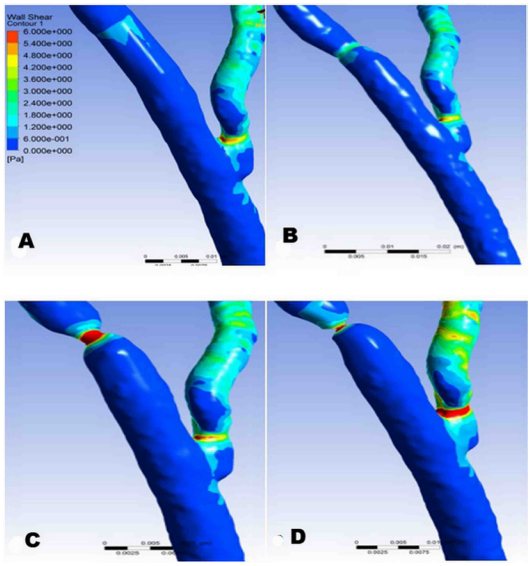

Figure 1: Wall shear stress distribution at proximal end-to-side anastomosis CCA to vein graft with various degrees of ICA stenosis, A) no stenosis, B) 30%, C) 70%, and D) 90% stenosis.

to be a Newtonian fluid, with constant viscosity (=4.0×10^{-3} Pa.s) and density (= 1060 kg/m^3). The Reynolds number in the normal ICA is 200 – 300, which is comparatively less than typical laminar flow of 1000 in any tubular structure. Therefore, laminar calculation was used in the study. The energy loss (EL), kinetic energy between inlet and outlet (including the pressure gradient and energy dissipation impacting into the vascular graft) were calculated by the equation (2), which is expressed below:

$$EL = \sum_{inlet}\left(P_{inlet} + \frac{1}{2}\rho u_{inlet}^2\right)Q_{inlet} - \sum_{outlet}\left(P_{outlet} + \frac{1}{2}\rho u_{outlet}^2\right)Q_{outlet} \quad (2)$$

The hemodynamic characteristics of brain bypass blood flow patterns were also quantified and their relationship with clinical decisions were explored. The anastomosis angle and the stenotic ratio of ICA, were modified by using image software. The hemodynamic characteristics of WSS distribution of proximal and distal anastomosis, and blood flow rate, through the graft and MCA borderzone, were simulated under the various anastomosis angles and ICA stenosis.

RESULTS

On the computational simulation, when the ICA had less than 60% area stenosis (Figure 2), there was normal volume of flow in the ICA and no flow in the bypass. Beyond 60% stenosis, the blood flow within the bypass linearly increased with the degree of ICA stenosis and the flow in the ICA linearly decreased. With an increase in bypass flow, there was a significant increase in WSS at the heel region of the bypass. Similar patterns of energy loss and WSS at the proximal and distal vein graft anastomosis were also observed as the degree of ICA stenosis increased.

Further analysis of the angle of anastomosis was performed. We used the 90% ICA stenosis on which we based our model, as this was the degree of stenosis that is used clinically for this bypass procedure. Various angles were simulated at the proximal and distal anastomosis. For proximal anastomosis (CCA to vein), anastomosis angles of 30, 45 and 90 degrees were modeled for WSS distribution (Figure 3). These anastomoses were characterized by flow acceleration into the proximal anastomosis marked by a moderate rise in WSS magnitude. This was most profoundly evident at the heel region of the proximal anastomosis. The peak WSS, energy loss and flow ratio between the CCA and bypass segment

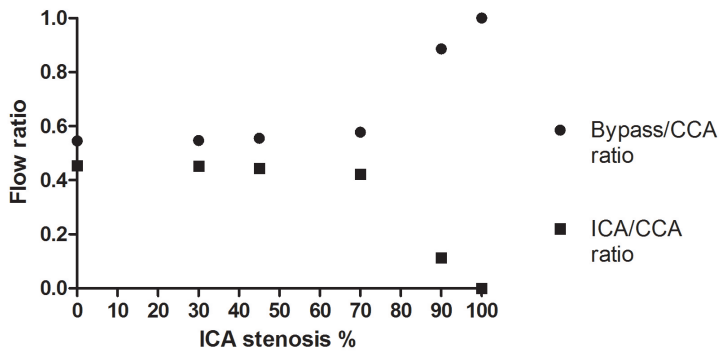

Figure 2: Blood flow distribution in ICA and bypass graft with various degrees of ICA stenosis.

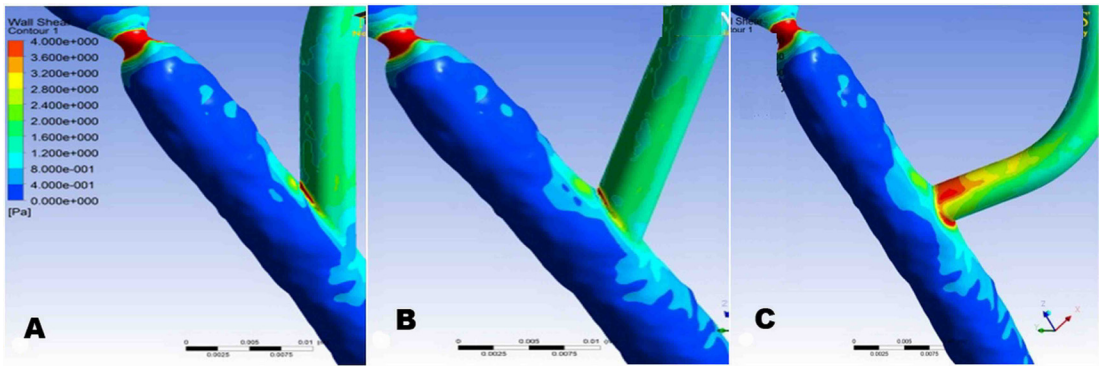

Figure 3. Wall shear stress distribution at the proximal anastomosis (CCA to vein) with various degrees of anastomosis angle, A) 30, B) 45 and C) 90.

were, however, relatively constant and were not related to the angle of the anastomosis (Figure 4). At the intracranial distal anastomosis (vein to MCA), angles were varied over 150, 135, 90 and 45 degrees to evaluate the effect on the distal anastomosis hemodynamics (Figure 5). There was evidence of flow separation with development of a retrograde shear vector, particularly evident in the anastomosis segment that was vein graft. Despite the inflow separation with retrograde shear vector, we observed there was no major influence on peak WSS or flow changes in the middle cerebral artery borderzone region with these varying angles of the distal anastomosis. Normalized shear rate along the upstream of the middle cerebral arterial wall were relatively constant throughout various angles of distal anastomosis in 90% ICA stenosis, as well as in the model of complete ICA occlusion (Figure 6).

DISCUSSION

Application of CFD as a tool for studying patient-specific hemodynamics is gaining in popularity. Numerous CFD clinical applications, particularly predicting the thrombosis rate in endovascular treatment of aneurysm and rupture risk of cerebral aneurysms, have been described.[16-18] Since the blood flow distribution and velocity profiles near the vascular bifurcation depend strongly on the geometry, it has been suggested that certain geometries (e.g. high curvature, obtuse and large angle of anastomosis) would alter the velocity profile, leading to more flow separation and low WSS. These geometric configurations, therefore, might be predisposed to early graft failure due to thrombosis, in the short-term, and to atherosclerosis and intimal hyperplasia, in the long-term. We set out to use high resolution data sets obtained from CTA combined with a robust computational fluid approach to study anastomosis angles in EC-IC brain bypass and perfusion at the borderzone area.

Flow dynamics and distribution

On the carotid artery computational simulation, we showed the outflow ratio changes in the carotid bifurcation from CCA to the ICA, ECA and vein bypass graft when the area of stenosis exceeds

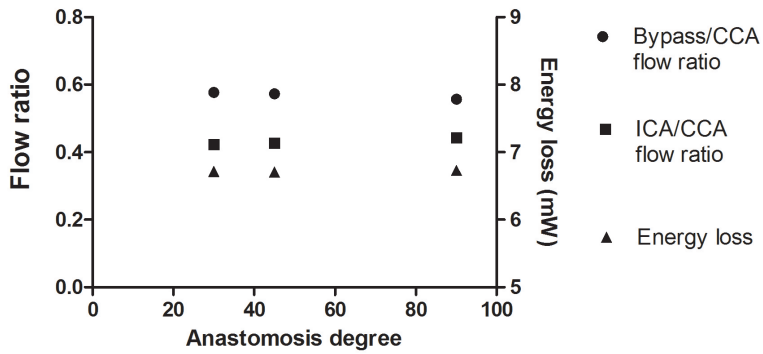

Figure 4. Energy loss, flow distribution at ICA and vein bypass segment at proximal anastomosis with various anastomosis angles.

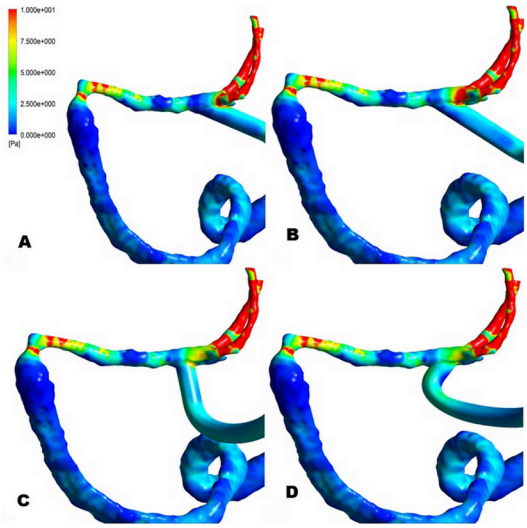

Figure 5. WSS distribution at distal anastomosis and M1 borderzone at A) 150, B) 135, C) 90 and D) 45 degrees end to side anastomosis with complete ICA occlusion.

60% (Figure 1 and Figure 2). Beyond 60%, further narrowing of ICA will result in increasing flow within the bypass. This increase was linearly related to the degree of stenosis beyond 60%. This is to be expected from both the theoretical and the experimental evidence but has yet to be investigated by CFD modeling.[19] Clinically, this degree of stenosis in the ICA has been found to be necessary before a benefit can be obtained by carotid endarterectomy.[20-23] This supports the likelihood that the benefits from carotid endarterectomy relate to a mechanical alteration in flow dynamics rather than removing the lesion generating the source of emboli.

Schirmer and Malek[11] employed similar modeling strategies to investigate the interaction between hemodynamic insufficiency, thromboembolism and complex blood flow patterns in intracranial atherosclerotic disease. They reported that intracranial arterial narrowing creates a hemodynamically pathological environment that favors platelet activation with embolus formation due, in part, to alterations in WSS. Flow rate of at least 40 cc/min are required to maintain a good patency rate.[7] The reasons for this relates to WSS. WSS is a flow-induced stress that can be described as the frictional force of viscous blood. Shear stress and local flow field play a critical role in determining where most vascular pathology originates.[24,25] This is particularly the case at the surgically created anastomosis bypass sites. Schirmer and Malek[11] revealed that abnormal stenosis or narrowing would create a hemodynamically pathological environment that favors platelet activation and abnormal shear stress. Recent studies have indicated the WSS changes, in space and time, affect endothelial cell function and alter local vascular tone, including nitric oxide(NO) elaboration, monocytes adhesion, and smooth muscle cell proliferation and migration.[26,27] Low and oscillatory WSS is regarded as a major factor in the development and growth of atherosclerotic and intimal hyperplasia in bypass grafts.[28] Intimal hyperplasia in vein grafts is sensitive to wall shear. Dobrin and colleagues[29] examined the hemodynamic mechanical factors, radial pressure extension and WSS on intimal hyperplasia in autogenous vein grafts on a canine's femoral artery. They observed intimal hyperplasia was less evident on the side with high flow (obtained by complete femoral artery ligation) as compared to the side where the femoral artery was left partially patent with low flow in the vein graft. Similar in-vitro findings were found in Kohler and Jawien's study[30] where intimal hyperplasia was significantly greater in rat CCA with a low flow

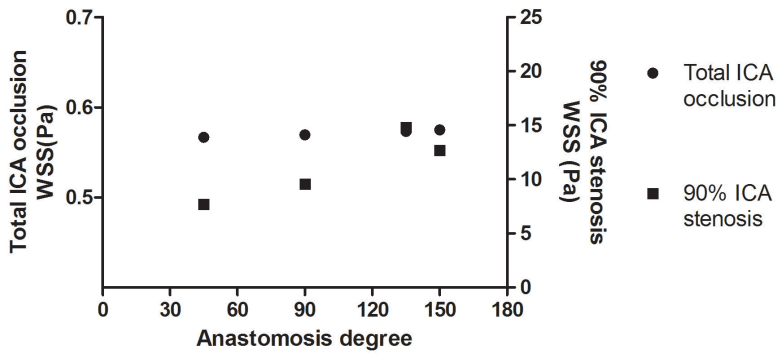

Figure 6: WSS distribution at distal anastomosis and M1 borderzone at 150, 135, 90 and 45 degrees end to side anastomosis with 90% stenosis and complete ICA occlusion.

group as compared with a high flow group. This is particularly pertinent in the case of bypass to the MCA where a point of low flow may occur in the region of the lenticulostriate arteries, at the point of borderzone between the bypass flow and the native collaterals for the planned occluded artery.[5] Internal borderzone infarctions may result from occlusion due to these hemodynamic changes.

Based on the computational modeling, we observed there was no major influence on WSS or flow changes in the middle cerebral artery borderzone (between the native circulation and that of the bypass) with differing angles of the distal anastomosis. This was the case despite the inflow separation with retrograde shear vector. CFD result revealed hemodynamic indices at the borderzone were not sensitive to various anastomosis angles. In this case, the absence of any WSS difference with varying angles of the distal bypass anastomosis may be due to lack of inflow influence from both the ipsilateral hypoplastic A1 and posterior communicating artery.

Limitations

Our current modeling technique has limitations as it assumes a rigid congruent bypass conduit and does not take into account vessel wall thickness, elastic properties, pulsatility, or complex temporal flow pattern changes in the Circle of Willis. Included in this complex temporal flow pattern is flow from the posterior circulation that may have a phase difference, and retrograde flow during parts of the cardiac cycle. In order to decrease computational time, our simulation study is based on a number of simplifying assumptions including considering blood as a Newtonian fluid as well as neglecting the effect of wall movement, gravity and position. However, the fluid solid interface (FSI) model from cardiac gated images is more realistic than the rigid model. We used a mean velocity waveform derived from carotid Doppler that may not represent the pulsatile waveform in patients with EC-IC bypass. Although it would be desirable to obtain in-vivo velocity data that can be coupled with the patient's bypass geometry, such data were not feasible. Furthermore, study of the distribution of hemodynamic forces in bypass graft has always been hampered by the complexity of intracranial vasculature, particularly at the carotid siphon area. Meticulous skeletonizing of the extraluminal ICA surface for computational modeling at the carotid siphon is mandatory.

In conclusion, image-based patient-specific computational models combined with information from other imaging modalities can be used in an efficient manner that allows clinical studies of brain bypass hemodynamics. Improved modeling approaches may help elucidate the mechanism for graft thrombosis and graft failure after brain bypass surgery. This modeling not only assists the quantification of the flow distribution, WSS and pressure gradient in brain bypass surgery, it may also provide a foundation in the understanding of hemodynamic stress and the pathophysiology of brain vascular disease. This technique may prove to be of value when planning bypass surgery to assist the prediction of graft failure.

ACKNOWLEDGEMENTS

One or more of the authors of this paper is supported by University of Malaya's HIR-MOHE research grant initiative (UM.C/625/1/HIR-MOHE/12) and University of Malaya Research Grant (UMRG) RG455-12HTM. The author would also like to thank Ms Elisa Yoke Kuan Lim for her analysis revision and manuscript preparation.

DISCLOSURE

Conflict of interest: None

REFERENCES

1. Sia SF, Davidson AS, Assaad NN, Stoodley M, Morgan MK. Comparative patency between intracranial arterial pedicle and vein bypass surgery. *Neurosurgery* 2011; 69:308-14.
2. Jeffree RL, Stoodley MA. STA-MCA bypass for symptomatic carotid occlusion and haemodynamic impairment. *J Clin Neurosci* 2009; 16:226-35.
3. Morgan MK, Brennan J, Day MJ. Interposition saphenous vein bypass graft between the common and intracranial internal carotid arteries. *J Clin Neurosci* 1996; 3:272-80.
4. Morgan MK, Ferch RD, Little NS, Harrington TJ. Bypass to the intracranial internal carotid artery. *J Clin Neurosci* 2002; 9:418-24.
5. Morgan MK, Morgan DK. Cerebral Revascularization. In: Kaye A, Black P, eds: Operative Neurosurgery, Vol 2. Sydney: Harcourt 2000:1163-78.
6. Morgan MK, Sekhon LH. Extracranial-intracranial saphenous vein bypass for carotid or vertebral artery dissections: a report of six cases. *J Neurosurg* 1994; 80:237-46.
7. Sundt TM, 3rd, Sundt TM, Jr. Principles of preparation of vein bypass grafts to maximize patency. *J Neurosurg* 1987; 66:172-80.
8. Haruguchi H, Teraoka S. Intimal hyperplasia and hemodynamic factors in arterial bypass and arteriovenous grafts: a review. *J Artif Organs* 2003; 6:227-35.
9. Ruggeri ZM. Platelets in atherothrombosis. *Nat Med* 2002;8:1227-34.

10. Ruggeri ZM, Dent JA, Saldivar E. Contribution of distinct adhesive interactions to platelet aggregation in flowing blood. *Blood* 1999;94:172-8.
11. Schirmer CM, Malek AM. Prediction of complex flow patterns in intracranial atherosclerotic disease using computational fluid dynamics. *Neurosurgery* 2007; 61:842-51; discussion 852.
12. Staalsen NH, Ulrich M, Kim WY, Pedersen EM, How TV, Hasenkam JM. In vivo analysis and three-dimensional visualisation of blood flow patterns at vascular end-to-side anastomoses. *Eur J Vasc Endovasc Surg* 1995; 10:168-81.
13. Qian Y, Liu JL, Itatani K, Miyaji K, Umezu M. Computational hemodynamic analysis in congenital heart disease: simulation of the Norwood procedure. *Ann Biomed Eng* 2010; 38:2302-13.
14. Sia SF, Qian Y, Matsuda W, Avolio A, Morgan M. Evaluation of brain extracranial-to-intracranial bypass treatments by using computational hemodynamic technology. In: Lim CT, Goh JCH, eds: World Congress of Biomechanics (WCB 2010), Vol 31. Singapore: Springer 2010:1542-5.
15. Jamali AA, Deuel C, Perreira A, Salgado CJ, Hunter JC, Strong EB. Linear and angular measurements of computer-generated models: are they accurate, valid, and reliable? *Comput Aided Surg* 2007; 12:278-85.
16. Xu BN, Wang FY, Lui L, Zhang XJ, Ju HY. Hemodynamics model of fluid-solid interaction in internal carotid artery aneurysms. *Neurosurg Rev* 2011; 34:39-47.
17. Shojima M, Oshima M, Takagi K, *et al*. Role of the bloodstream impacting force and the local pressure elevation in the rupture of cerebral aneurysms. *Stroke* 2005; 36:1933-8.
18. Cebral JR, Castro MA, Burgess JE, Pergolizzi RS, Sheridan MJ, Putman CM. Characterization of cerebral aneurysms for assessing risk of rupture by using patient-specific computational hemodynamics models. *AJNR Am J Neuroradiol* 2005; 26:2550-9.
19. Nichols WW, O'Rourke MF. Contours of pressure and flow waves in arteries. McDonald's Blood Flow In Arteries. Theoretical, Experimental and Clinical Principles. London: Hodder Arnold 2005:186-7.
20. Collaborators NASCET. Beneficial effect of carotid endarterectomy in symptomatic patients with high-grade carotid stenosis. *N Engl J Med* 1991; 325:445-53.
21. Group ECSTC. MRC European Carotid Surgery Trial: interim results for symptomatic patients with severe (70-99%) or with mild (0-29%) carotid stenosis. . *Lancet* 1991; 337:1235-43.
22. Investigators NASCETN. Clinical alert: benefit of carotid endarterectomy for patients with high-grade stenosis of the internal carotid artery. National Institute of Neurological Disorders and Stroke Stroke and Trauma Division. *Stroke* 1991; 22:816-7.
23. Investigators NASCETN. North American Symptomatic Carotid Endarterectomy Trial. Methods, patient characteristics, and progress. *Stroke* 1991; 22:711-20.
24. Davies PF. Hemodynamic shear stress and the endothelium in cardiovascular pathophysiology. *Nat Clin Pract Cardiovasc Med* 2009; 6:16-26.
25. Glagov S, Zarins C, Giddens DP, Ku DN. Hemodynamics and atherosclerosis. Insights and perspectives gained from studies of human arteries. *Arch Pathol Lab Med* 1988; 112:1018-31.
26. Davies PF, Barbee KA, Lal R, Robotewskyj A, Griem ML. Hemodynamics and atherogenesis. Endothelial surface dynamics in flow signal transduction. *Ann N Y Acad Sci* 1995; 748:86-102; discussion 102-3.
27. White CR, Haidekker M, Bao X, Frangos JA. Temporal gradients in shear, but not spatial gradients, stimulate endothelial cell proliferation. *Circulation* 2001; 103:2508-13.
28. Westerhof N, Stergiopulos N, Noble MIM. Blood flow and arterial disease. In: Westerhof N, Stergiopulos N, Noble MIM, eds: Snapshots of Hemodynamics. An aid for clinical research and graduate education. Boston: Springer 2005:143.
29. Dobrin PB, Littooy FN, Endean ED. Mechanical factors predisposing to intimal hyperplasia and medial thickening in autogenous vein grafts. *Surgery* 1989; 105:393-400.
30. Kohler TR, Jawien A. Flow affects development of intimal hyperplasia after arterial injury in rats. *Arterioscler Thromb* 1992; 12:963-71.